

A Parallel, Adaptive, First-Order System Least-Squares (FOSLS) Algorithm for Incompressible Resistive, Magnetohydrodynamics (MHD)

J. H. Adler*, T. Manteuffel†, S. McCormick†, J. Nolting†, J. Ruge† and L. Tang†

**Tufts University
Department of Mathematics
Medford, MA*

*†University of Colorado at Boulder
Department of Applied Mathematics
Boulder, CO*

Keywords: magnetohydrodynamics, adaptive mesh refinement, algebraic multigrid, nested iteration
PACS: 52.65.Kj, 02.70.-c

INTRODUCTION

Magnetohydrodynamics (MHD) is a model of plasma physics that treats the plasma as a charged fluid. As a result, the set of partial differential equations that describe this model are a time-dependent, nonlinear system of equations. Thus, the equations can be difficult to solve and efficient numerical algorithms are needed. This work shows the use of such an efficient algorithm on the incompressible, resistive MHD equations. A first-order systems least-squares (FOSLS) [1, 2] finite element discretization is used along with nested iteration and algebraic multigrid (AMG) [3, 4, 5, 6, 7, 8]. The main focus of this work is to show that if a nested iteration algorithm along with an efficiency-based adaptive mesh refinement (AMR) scheme is used, then a nonlinear system of equations, such as the MHD equations, can be solved in only a handful of work units per time step. Here, a work unit is defined as the equivalent of one relaxation sweep on the finest grid. In other words, the accuracy-per-computational-cost for solving the MHD equations can be maximized by the use of nested iteration and AMR. An island coalescence instability was able to be resolved in less than 10 work units per time step. Further details of this work can be found in several companion papers. In [9], the FOSLS method applied to MHD is described. The nested iteration algorithm has also been developed in [10] and [11] and the efficiency-based AMR method known as ACE, is discussed in [12, 13, 14, 15].

THE MHD EQUATIONS AND FOSLS FORMULATION

The resistive MHD equations are a coupling of the incompressible Navier-Stokes and Maxwell's systems. The primitive variables are defined to be the fluid velocity, \mathbf{u} , the fluid pressure, p , the magnetic field, \mathbf{B} , the current density, \mathbf{j} , and the electric field, \mathbf{E} . In addition, a resistive form of Ohm's law, $\mathbf{j} = \sigma(\mathbf{E} + \mathbf{u} \times \mathbf{B})$, is used to eliminate the electric field, \mathbf{E} , from the equations. The equations are non-dimensionalized using Alfvén units and the constants R_e (fluid Reynolds Number) and S_L (Lundquist Number) are assumed constants, which are adjusted for different types of physical behavior [16, 17].

Using the FOSLS method [1, 2], the system is first put into a differential first-order system of equations. This is done based on a vorticity-velocity-pressure-current formulation [18, 19, 20]. A scaling analysis is performed in [9] for the full MHD system. The resulting scaling yields a nice block structure of the MHD system, which results in good AMG convergence of the linear systems obtained, while still preserving the physics of the system.

Vorticity, $\boldsymbol{\omega} = \nabla \times \mathbf{u}$, is introduced and the final formulation in 3D is

$$\frac{1}{\sqrt{R_e}} \nabla \times \mathbf{u} - \sqrt{R_e} \boldsymbol{\omega} = 0, \quad (1)$$

$$\frac{1}{\sqrt{R_e}} \nabla \cdot \mathbf{u} = 0, \quad (2)$$

$$\sqrt{R_e} \nabla \cdot \boldsymbol{\omega} = 0, \quad (3)$$

$$\frac{1}{\sqrt{R_e}} \frac{\partial \mathbf{u}}{\partial t} - \mathbf{u} \times \boldsymbol{\omega} - \mathbf{j} \times \mathbf{B} - \sqrt{R_e} \nabla p + \frac{1}{\sqrt{R_e}} \nabla \times \boldsymbol{\omega} = \mathbf{f}, \quad (4)$$

$$\frac{1}{\sqrt{S_L}} \nabla \times \mathbf{B} - \sqrt{S_L} \mathbf{j} = 0, \quad (5)$$

$$\frac{1}{\sqrt{S_L}} \nabla \cdot \mathbf{B} = 0, \quad (6)$$

$$\sqrt{S_L} \nabla \cdot \mathbf{j} = 0, \quad (7)$$

$$\frac{1}{\sqrt{S_L}} \frac{\partial \mathbf{B}}{\partial t} + \frac{1}{\sqrt{R_e S_L}} (\mathbf{u} \cdot \nabla \mathbf{B} - \mathbf{B} \cdot \nabla \mathbf{u}) + \frac{1}{\sqrt{S_L}} \nabla \times \mathbf{j} = \mathbf{g}. \quad (8)$$

The above system is denoted by $\mathcal{L}(u) = f$, where $u = (\mathbf{u}, \boldsymbol{\omega}, p, \mathbf{B}, \mathbf{j})^T$ represents a vector of all of the dependent variables that should not be confused with the vector fluid velocity, \mathbf{u} . Then, the L^2 norm of the residual of this system is minimized. This is referred to as the nonlinear functional,

$$\mathcal{F}(u) = \|\mathcal{L}(u) - f\|_0. \quad (9)$$

In general, we wish to find the argmin of (9) in some solution space \mathcal{V} . Usually, \mathcal{V} is chosen to be an H^1 product space with boundary conditions that are chosen to satisfy the physical constraints of the problem as well as the assumptions needed for the FOSLS framework. In practice, a series of nested finite subspaces, \mathcal{V}^h , are used to approximate the solution in \mathcal{V} . However, in the Newton-FOSLS approach [21, 22], system (1)-(8) is first linearized using a Newton step before a FOSLS functional is formed and minimized. This results in the weak form of the problem that produces symmetric positive definite algebraic systems when the problem is restricted to a finite-dimensional subspace, \mathcal{V}^h . In addition, proving continuity and coercivity of the resulting bilinear form is equivalent to having H^1 equivalence of the FOSLS functional. Moreover, the FOSLS functional yields a sharp a posteriori local error estimate, which is used to make the algorithm more robust and, under the right conditions, produces algebraic systems that are solved easily by multilevel iterative solvers. Our choice here is algebraic multigrid (AMG) [3, 4, 5, 6, 7, 8], which, when applied to the FOSLS discretization, has been shown to be an optimal ($O(n)$) solver [1, 2, 6]. Using the formulation above, and with appropriate boundary conditions, H^1 equivalence of the linearized FOSLS functional is shown in [11]. Therefore, the FOSLS functionals can be a good measure of the error, or at least the semi-norm of the error, in the solution space. Thus, they can be used to develop an efficient solution algorithm and as aids in the adaptive refinement process. By measuring the functional norm of the error in each element of the domain, information on where refinement is needed is readily available.

SOLUTION ALGORITHM

In [10], an algorithm is devised to solve a system of nonlinear equations, $\mathcal{L}(u) = f$. Starting on a coarse grid, given an initial guess, the system is linearized and the linearized FOSLS functional is then minimized on a finite element space. At this point, several AMG V-cycles are performed until there is little to gain in accuracy-per-computational-cost. The system is then relinearized and the minimum of the new linearized FOSLS functional is searched for in the same manner. After each set of linear solves, the relative difference between the computed linearized functional and the nonlinear functional is checked. If they are close and near the minimum of the linearized functional, then it is concluded that we are close enough to the minimum of the nonlinear functional and, hence, we have a good approximation to the solution on the given grid. Next, the approximation is interpolated to a finer grid and the problem is solved on that grid. This process is repeated until an acceptable error has been reached, or until we have run out of computational resources, such as memory. If, as in the case of the MHD equations, it is a time-dependent problem, the whole process is performed at each time step. This algorithm is summarized in the following pseudocode.

Algorithm 1: Nested Iteration Newton-FOSLS AMG

```
for  $t = 1$  to max time step do
  Go to coarsest grid
  while fine grid resolution is not reached do
    for  $n = 1$  to max Newton step do
      Linearize first-order system
      Minimize FOSLS functional
      while functional of current approximation is large do
        | Solve  $Ax = b$  with AMG
      end
      Compute relative difference between linearized and nonlinear operator
      if small then
        | Exit Newton loop
      end
    end
    Refine grid
  end
  Update time step
end
```

Adaptive Refinement

In the nested iteration algorithm, we decide when to stay on a current mesh and iterate further or interpolate to a finer grid. On a given mesh, after enough Newton steps and linear iterations have been performed, the nonlinear functional is calculated in each element. This indicates in which region of the domain the functional and, hence, the error is large compared to the rest of the domain. Then, the best use of new degrees of freedom is to concentrate them where the error is large. Since the goal of the algorithm is to increase the accuracy-per-computational-cost, we do not want to over solve in areas where the error is already small. The adaptive scheme that we describe here is an efficiency based refinement method, called ACE, that was developed in [12, 13, 14]. This scheme estimates both the reduction in the functional and the computational cost that would result from any given refinement pattern. These estimates are used to establish a refinement pattern that attempts to optimize the Accuracy-per-Computational cost (Efficiency), which gives rise to the acronym ACE. This method applied in the nested iteration and FOSLS framework toward MHD can be found in [15].

The square of the functional value on each element, ε_i , is computed and is ordered such that the local functional value is decreasing, $\varepsilon_1 \geq \varepsilon_2 \geq \dots \geq \varepsilon_{N_l}$, where N_l is the total number of elements on level l . Next, we predict the reduction of the squared functional and the estimated computational work that would result if we were to refine a given percentage of the elements with the most error. Denote the percentage by $r \in (0, 1]$ and the number of elements to be refined by $r * N_l$. Therefore, we refine only $r * N_l$ elements on each level that gives us the best error reduction for the added cost.

In addition, one could allow for multiple refinements of each element. For example, the ACE scheme could call for $r_1 N_l$ elements to be refined once and $r_2 N_l$ elements to be refined twice. This changes the predicted error reduction and the predicted work estimate. Now, the optimal pair, (r_1, r_2) , is found to minimize the effective error reduction. This allows for more aggressive refinement. In practice, it has been found that using even more refinement, such as triple refinement, is unnecessary.

NUMERICAL RESULTS

The full algorithm described above was applied to a 2D reduced MHD tokamak test problem [23, 24, 25, 26]. These equations simulate a "large aspect-ratio" tokamak, with non-circular cross-sections. Here, the magnetic B-field along the z-direction, or the toroidal direction, is very large and mostly constant. In this context, we are able to look at plasma behavior in the poloidal cross-section.

This specific test problem simulates an island coalescence in the current density arising from perturbations in an initial current density sheet. A current density sheet in the toroidal direction of the tokamak is perturbed, resulting in

TABLE 1. Average number of work units per timestep using uniform refinement versus ACE refinement. A total of 100 time steps were performed.

Uniform		ACE		Work Ratio	Element Ratio
Work Units	Nonzeros	Work Units	Nonzeros		
66.87	51,781,975	78.23	7,283,047.4	0.16	0.07

an instability that causes a reconnection in the magnetic field lines and merging of two islands in the current density field. This produces a sharp peak in current density where the magnetic field lines reconnect. This region is known as the reconnection zone. See [27, 28, 25] for more details. We choose a low enough resistivity (i.e. Lundquist number above 50,000) in order to observe the interesting physics.

The problem was run to time $10\tau_A$ with a timestep of $0.1\tau_A$ using a BDF-2 implicit time-stepping scheme. By the 80th time step, or time $8\tau_A$, the islands have coalesced and the large peak in current density has occurred at the reconnection point. Using both uniform refinement and the ACE scheme, we were able to capture the instability. With ACE employed, the grids evolve over time to refine in areas with steeper gradients. In this problem, as time progresses, a steep gradient occurs at the reconnection point. This is seen in the bottom graph in figure 1. We expect, then, that most of the refinement occurs in this region, which is indeed the case.

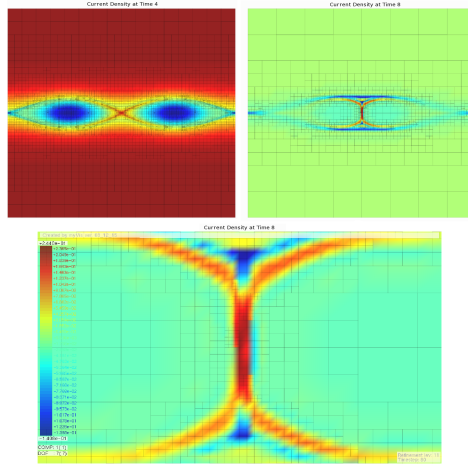


FIGURE 1. Numerical solution using 10 levels of adaptive refinement. $S_L = R_e = 50,001$. Top Left: Current Density at Time $4\tau_A$. Top Right: Current Density at Time $8\tau_A$. Bottom: Zoomed in plot of current density peak at Time $8\tau_A$.

Next, the work performed using ACE is compared to that of using uniform refinement. The work at one time step is calculated in terms of work units, which, again, is the equivalent of performing one Gauss-Seidel relaxation sweep on the finest grid used. All work units are based on the finest grid obtained from uniform refinement. Therefore, the Work Ratio column represents how much work the adaptive scheme did compared to the uniform scheme. Similarly, the Element Ratio column is the ratio of elements on the finest grid of the adaptive scheme compared to the number of elements on the finest grid of the uniform scheme.

The results show that using adaptive refinement greatly reduces the amount of work needed, compared to that of using uniform refinement as is done in [10]. ACE requires 10% of the work that uniform refinement requires. The physics is more localized in this problem, especially by time $8\tau_A$ and, thus, the refinement is more localized. Looking at one specific time step, as in table 2, one can see how the nested iteration algorithm along with ACE solves the problem efficiently. By the finest levels, only one Newton step and a handful of work units are needed. The values in parenthesis show the relative work with respect to a grid that was uniformly refined for the given number of levels. Thus, using nested iteration Newton-FOSLS-AMG with ACE yields a good approximation to the solution of the island coalescence problem in less than 10 work units, or the equivalent of 10 relaxation sweeps on a 128×128 bi-quadratic uniform grid.

TABLE 2. Results for a single time step. AMG convergence factor, ρ , total work units (total work units with respect to uniform refinement in parenthesis), and the nonlinear functional norm are given.

Level	Elements	Nonzeros	Newton Steps	ρ	Work Units	Nonlinear Functional
2	4	17,493	2	0.35	0.054 (0.006)	4.919
3	16	63,063	2	0.55	0.355 (0.038)	1.287
4	40	155,575	1	0.40	0.427 (0.046)	0.604
5	79	299,145	1	0.46	0.682 (0.073)	0.284
6	175	640,871	1	0.58	3.328 (0.356)	0.112
7	337	1,161,741	1	0.50	3.929 (0.420)	0.049
8	658	2,263,261	1	0.79	19.548 (2.090)	0.023
9	1,078	3,624,089	1	0.67	20.789 (2.222)	0.013
10	1,696	5,535,089	1	0.71	29.495 (3.153)	0.008
			Total		78.697 (8.398)	

ACKNOWLEDGMENTS

This work was sponsored by the Department of Energy under grant numbers DE-FG02-03ER25574 and DE-FC02-06ER25784, Lawrence Livermore National Laboratory under contract numbers B568677, and the National Science Foundation under grant numbers DMS-0621199, DMS-0749317, and DMS-0811275.

REFERENCES

1. Z. Cai, R. Lazarov, T. Manteuffel, and S. McCormick, *SIAM J. Numer. Anal.* **31**, 1785–1799 (1994).
2. Z. Cai, T. Manteuffel, and S. McCormick, *SIAM J. Numer. Anal.* **34**, 425–454 (1997).
3. A. Brandt, S. F. McCormick, and J. Ruge, Algebraic Multigrid (AMG) for automatic multigrid solutions with application to geodetic computations, Report, Inst. for Computational Studies, Fort Collins, CO (1982).
4. A. Brandt, S. F. McCormick, and J. Ruge, *Algebraic Multigrid (AMG) for sparse matrix equations*, Cambridge University Press, 1984.
5. A. Brandt, *Appl. Math. Comput.* **19**, 23–56 (1986), ISSN 0096-3003.
6. W. L. Briggs, V. E. Henson, and S. F. McCormick, *A Multigrid Tutorial*, Society for Industrial and Applied Mathematics (SIAM), Philadelphia, PA, 2000.
7. C. Oosterlee, A. Schuller, and U. Trottenberg, *Multigrid*, Academic Press, 2000.
8. J. Ruge, and K. Stüben, *Algebraic Multigrid (AMG)*, Multigrid Methods (McCormick, S.F., ed), 1986.
9. J. Adler, T. Manteuffel, S. F. McCormick, and J. Ruge, *SIAM J. Sci. Comp.* **to appear** (2009).
10. J. Adler, T. Manteuffel, S. McCormick, J. Ruge, and G. Sanders, *SIAM J. on Sci. Comp. (SISC)* (submitted 2009).
11. J. Adler, *Nested Iteration and First Order Systems Least Squares on Incompressible Resistive Magnetohydrodynamics*, Ph.D. thesis, University of Colorado at Boulder (2009).
12. M. Berndt, T. Manteuffel, and S. F. McCormick, *E.T.N.A.* **6**, 35–43 (1998).
13. H. DeSterck, T. Manteuffel, S. McCormick, J. Nolting, J. Ruge, and L. Tang, *J. Num. Lin. Alg. Appl.* **15**, 249–270 (2008).
14. J. Nolting, *Efficiency-based Local Adaptive Refinement for FOSLS Finite Elements*, Ph.D. thesis, University of Colorado at Boulder (2008).
15. J. H. Adler, T. A. Manteuffel, S. F. McCormick, J. W. Nolting, J. W. Ruge, and L. Tang, *SIAM J. Sci. Comput.* **33**, 1–24 (2011), URL <http://link.aip.org/link/?SCE/33/1/1>.
16. D. R. Nicholson, *Introduction to Plasma Theory*, John Wiley and Sons, New York, 1983.
17. P. Ullrich, Dynamics and Properties of the Magnetohydrodynamics Equations (2005), unpublished.
18. P. Bochev, Z. Cai, T. Manteuffel, and S. McCormick, *SIAM J. Numer. Anal.* **35**, 990–1009 (1998).
19. P. Bochev, Z. Cai, T. Manteuffel, and S. McCormick, *SIAM J. Numer. Anal.* **36**, 1125–1144 (1999).
20. J. Heys, E. Lee, T. Manteuffel, and S. McCormick, *J. Comp. Phys.* **226**, 994–1006 (2007).
21. A. Codd, *Elasticity-Fluid Coupled Systems and Elliptic Grid Generation (EGG) Based on First-Order System Least Squares (FOSLS)*, Ph.D. thesis, University of Colorado at Boulder (2001).
22. A. Codd, T. Manteuffel, and S. McCormick, *SIAM J. Numer. Anal.* **41**, 2197–2209 (2003).
23. L. Chacon, D. A. Knoll, and J. M. Finn, *J. of Computational Physics* **178**, 15–36 (2002).
24. L. Chacon, D. A. Knoll, and J. M. Finn, *Physics of Plasmas* **9**, 1164–1176 (2002).
25. B. Philip, L. Chacon, and M. Pernice, *J. Comp. Phys.* **227**, 8855–8874 (2008).
26. H. Strauss, *Physics of Fluids* **19**, 134–140 (1976).
27. G. Bateman, *MHD Instabilities*, The MIT Press, 1978.
28. D. A. Knoll, and L. Chacon, *Physics of Plasmas* **13** (2006).